DOI 10.1007/s11595-017-1770-z

Hot Deformation Behavior of AZ40 Magnesium Alloy at Elevated Temperatures

LAI Lin, ZHANG Kui*, MA Minglong, LI Xinggang, LI Yongjun, SHI Guoliang, YUAN Jiawei

(State Key Laboratory for Fabrication and Processing of Nonferrous Metals, Beijing General Research Institute for Nonferrous Metals, Beijing 100088, China)

Abstract: Hot compression tests on AZ40 magnesium alloy were conducted on a Gleeble 1500d hot simulation testing machine in a deformation temperature range of 330 ℃-420 ℃ and a strain rate range of 0.002-2 s^{-1}. Hot deformation behaviors were investigated on the basis of the analysis of the flow stress-strain curves, constitutive equation, and processing map. The stress exponent and apparent activation energy were calculated to be 5.821 and 173.96 kJ/mol, respectively. Deformation twins and cracks located in grain boundaries were generated at 330 ℃ and 0.02 s^{-1}, which are associated with a high strain rate and a limited number of available slip systems. With increasing temperature and decreasing strain rate, the twins disappeared and the degree of dynamic recrystallization increased. The alloy was completely dynamically recrystallized at 420 ℃ and 0.002 s^{-1}, with a homogenous grain size of approximately 13.7 μm. The instability domains of the deformation behavior can be recognized by processing maps. By considering the processing maps and characterizing the microstructure, the optimum hot deformation parameters in this experiment were determined to be 420 ℃ and 0.002 s^{-1}.

Key words: AZ40 magnesium alloy; hot compression; processing map; recrystallization

1 Introduction

Given their high specific strength and specific stiffness, magnesium alloys show good potential for structural applications in aerospace and vehicle manufacturing[1]. However, the applications of magnesium alloys have been limited by disadvantages, such as relatively low strengths compared with steel or aluminum alloys and poor formability at room temperature because of the limited number of operative slip systems[2-5]. One of the most effective ways to enhance the room temperature strength and ductility of magnesium alloys is grain refinement by dynamic recrystallization (DRX). DRX easily occurs in magnesium alloys during hot deformation because of the lower stacking fault energy. To control the deformation of microstructures, the plastic forming ability and mechanical properties of magnesium alloys by DRX should be improved. The recrystallization of fine grains during hot deformation has been applied to produce commercial magnesium alloy components[6-8].

Several studies focused on issues specific to the deformation of AZ serial magnesium alloys. Srinivasan *et al*[9] investigated the hot deformation behavior of the binary as-cast Mg-3Al alloy via the processing-map technique. Their work highlighted the relevance of mechanisms such as DRX, grain boundary sliding, and dynamic recovery under limited deformation conditions. Their group reported that grain boundary sliding is responsible for the high efficiency domain of the processing map that occurs below 10^{-3} s^{-1} and spreads over 350 ℃-450 ℃. Xu *et al*[10] studied the influence of the initial microstructure and temperature on the deformation behavior of AZ91 magnesium alloys and aimed to save on manufacturing costs by directly using the as-cast materials without homogenization for hot working. Only a few groups have focused on the hot deformation behavior of the AZ40 alloy. Wang *et al*[11] studied the effect of hot rolling on grain refining and the mechanical properties of AZ40 magnesium alloy. Their group reported that after five or more rolling passes, the grain size is reduced to less than 10 μm, whereas the yield strength and tensile elongation of the AZ40 magnesium alloy sheets achieve as much as 175 MPa and 20% in the rolling and transverse directions. Given the low content of additional alloying

(Received: Sep. 20, 2016; Accepted: Nov. 12, 2016)

LAI Lin (赖林):Ph D; E-mail: lailin0125@126.com

*Corresponding author: ZHANG Kui (张奎): Prof.; Ph D; zhkui@grinm.com

Funded by the National Natural Science Foundation of China(No.51204020), the National Program on Key Basic Research Project (No 2013CB632202), and the Qinghai Provincial Science and Technology Support Project (2014-GX-106A)

elements, the solidification segregation of the AZ40 magnesium alloy is not serious. Thus, the feasibility of processing, such as forging and extrusion, directly with the as-cast alloy was explored; the improved production efficiency by reducing the material molding process is highly necessary and attractive. The aim of the present investigation is to study the hot deformation behavior of the as-cast AZ40 magnesium alloy by compression tests, combined with flow curves and DRX evolution analysis, to establish a methodology to optimize deformation techniques.

2 Experimental

The material investigated in this study was an AZ40 alloy prepared by semi-continuous casting. The chemical composition of the alloy tested by the ARL4460 optical spectrometer was Al, 3.98wt%; Zn, 0.40wt%; Mn, 0.2wt%; and balance Mg. Fig.1 shows the microstructures of the as-cast AZ40 alloy specimen used in this study. The as-cast alloy specimen exhibited a typical discontinued net eutectic microstructure, and the second phase was mainly distributed in the grain boundaries.

From the as-cast billet, cylindrical compression test specimens of 10 mm in diameter and 15 mm in height were machined according to ASTM: E209. The specimens were extruded in the temperature range of 330 ℃-410 ℃ and the strain rate range of 0.002-2 s^{-1} in a Gleeble 1500 thermomechanical simulator. All the specimens were compressed to a true strain of 0.916. Before compression, the specimens were heated

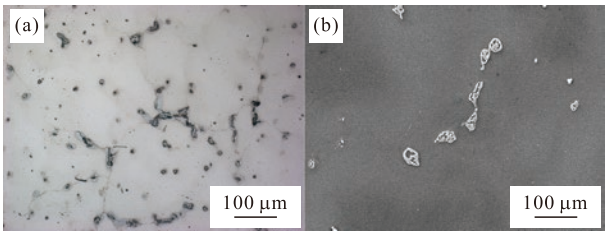

Fig.1 Typical microstructures of the as-cast AZ40 alloy specimen: (a) Optical microstructure; (b) SEM image

to the test temperature at a rate of 5 ℃/s and held for 3 min to obtain a stable and uniform deformation temperature. To reduce the friction, the slices of graphite were applied to the top and bottom surfaces of each sample. After compression, all the specimens were water quenched to preserve the microstructure. For metallographic examination, the deformed specimens were sectioned parallel to the deformation axis, whereas the cut surface was mounted, polished, and etched using a 2 mL solution of nitric acid and 98 mL of ethanol.

3 Results and discussion

3.1 Flow curves

A series of typical true stress-strain curves of the AZ40 magnesium alloy were obtained at various temperatures and different strain rates, which are presented in Fig.2. The flow stress increases up to a peak value at a certain strain and then decreases to a relatively steady state with increasing strain until the end of compression. This step presents a typical characteristic of hot working accompanied by strain

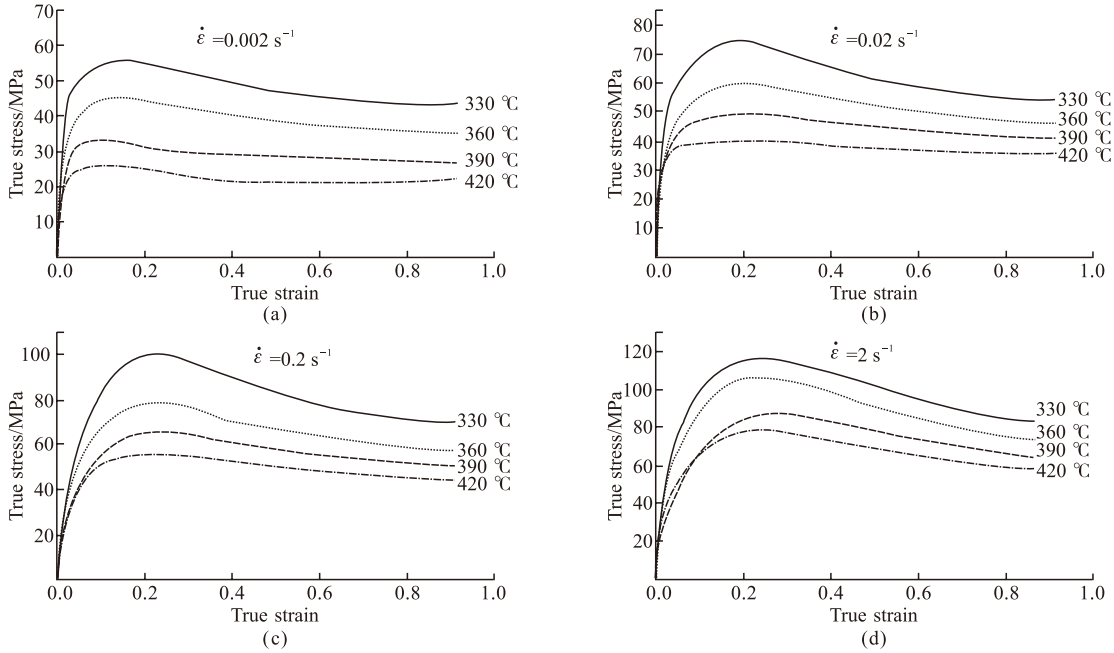

Fig.2 True stress-strain curves for the AZ40 alloy under various compression deformation conditions: (a) $\dot{\varepsilon}$=0.002 s^{-1}; (b) $\dot{\varepsilon}$=0.02 s^{-1}; (c) $\dot{\varepsilon}$=0.2 s^{-1}; (d) $\dot{\varepsilon}$=2 s^{-1}

hardening and dynamic softening[12]. In addition, the flow stress decreases as the deformation temperature increases or as the strain rate decreases.

3.2 Constitutive equation

According to the hot deformation test of the as-extruded Mg-Gd-Y-Zn-Zr alloy by Xia[13], the relationship between the steady-state flow stress, the deformation temperature, and the strain rate of the materials during hot working can be commonly expressed by the hyperbolic sine-type Arrhenius equation over a wide range of temperatures and strain rates as follows:

$$\dot{\varepsilon} = A[\sinh(\alpha\sigma)]^n \exp[-Q/(RT)] \quad (1)$$

at a low stress level ($\alpha\sigma < 0.8$) or a high stress level ($\alpha\sigma > 1.2$), the relationship of the flow stress with the deformation temperature and strain rate can be described by exponential laws as shown in Eqs.(2) and (3), respectively:

$$\dot{\varepsilon}=A_1\sigma^{n_2}\exp[-Q/(RT)] \quad (2)$$

$$\dot{\varepsilon}=A_2\exp(\beta\sigma)\exp[-Q/(RT)] \quad (3)$$

where, $\dot{\varepsilon}$ is the strain rate; σ is the flow stress; Q is the activation energy of deformation; R is the gas constant of 8.314 J/K·mol; T is the deformation temperature; and A, A_1, A_2, n, n_1, β, and α ($\alpha = \beta/n_1$) are the constants independent of σ and T.

Eqs.(1)-(3) can be expressed as follows by applying natural logarithms of both sides of the equations:

$$\ln\dot{\varepsilon} = \ln A - \frac{Q}{RT} + n\ln[\sinh(\alpha\sigma)] = \ln B + n\ln[\sinh(\alpha\sigma)] \quad (4)$$

$$\ln\dot{\varepsilon}=\ln B_1+n_1\ln\sigma \quad (5)$$

$$\ln\dot{\varepsilon}=\ln B_2+\beta\sigma \quad (6)$$

According to the peak stress at different temperatures, the linear relationships of ln σ-ln$\dot{\varepsilon}$ and σ-ln$\dot{\varepsilon}$ were fitted, as shown in Fig.3. The correlation coefficients of monadic linear regression are greater than 0.97. In Fig.3(a), the value of n_1 can be calculated as 7.08765 by the linear regression of (ln σ-ln$\dot{\varepsilon}$) at low stress levels (the average of the gradient of line 390 ℃ and line 420 ℃). In Fig. 3(b), the value of β is 0.112365, which was obtained through the linear regression of (σ-ln$\dot{\varepsilon}$) at a high stress level (the average of the gradient of line 330 ℃ and line 360 ℃). In Fig.3(c), $\alpha = \beta/n_1$, where n was calculated to be 5.821 by the linear regression of (ln [sin h ($\alpha\sigma$) - ln $\dot{\varepsilon}$]).

Based on the assumption that the deformation activation energy has no correlation with T, the activation energy Q can be expressed as follows:

$$Q = R\left.\frac{\partial\ln\dot{\varepsilon}}{\partial\ln[\sinh(\alpha\sigma)]}\right|_T \cdot \left.\frac{\partial\ln[\sinh(\alpha\sigma)]}{\partial(1/T)}\right|_{\dot{\varepsilon}} \quad (7)$$

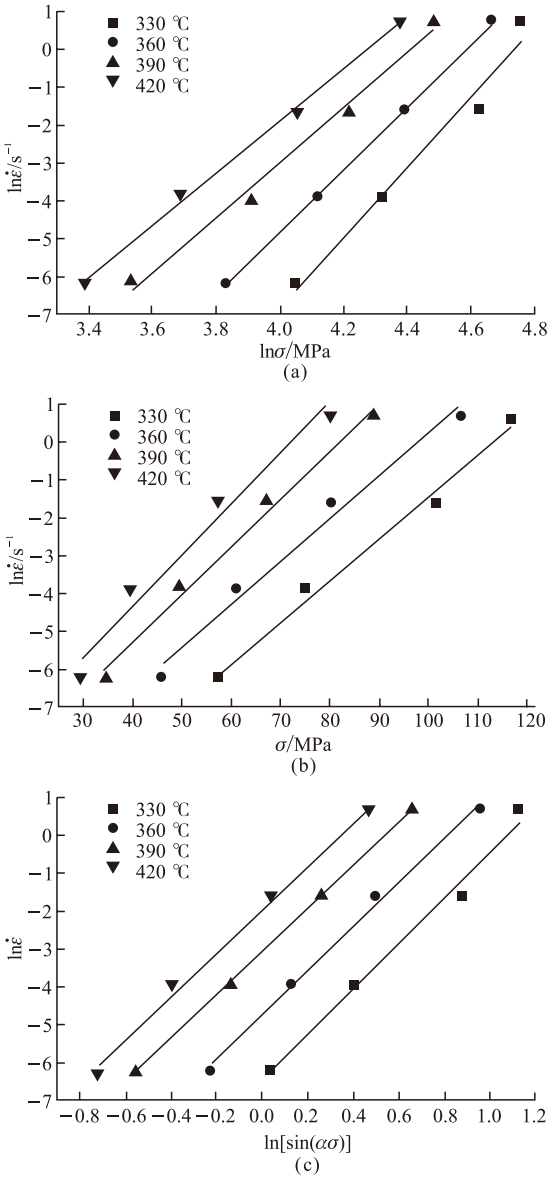

Fig.3 Relationship between ln$\dot{\varepsilon}$ and (a) lnσ; (b) σ; (c) ln[sin($\alpha\sigma$)]

where $\left.\frac{\partial\ln\dot{\varepsilon}}{\partial\ln[\sinh(\alpha\sigma)]}\right|_T$ stands for the slope of ln [sin h ($\alpha\sigma$)] $-\ln\dot{\varepsilon}$ (the value of n) and $\left.\frac{\partial\ln[\sinh(\alpha\sigma)]}{\partial(1/T)}\right|_{\dot{\varepsilon}}$ stands for the slope of ln [sin h ($\alpha\sigma$)] - 1/T. Fig. 4 shows the relationship between ln [sin h ($\alpha\sigma$)] and 1/T with different strain rates, thereby evaluating the averaged activation energy. The linearly dependent coefficients for ln [sin h ($\alpha\sigma$)] - 1/T are all greater than 0.97. The average activation energy Q is calculated to be 173957.6 J/mol by combining the results of Figs.3(c) and 4.

From Eq.(4), the intercept of the ln [sin h ($\alpha\sigma$)] - 1/T

fitted curve is $\ln A - \frac{Q}{RT}$. After the values of Q, R, and T are substituted, A can be calculated as the average value of 1.987×10^{12} s^{-1}. Thus, the flow stress of the AZ40 magnesium alloy during hot compressive deformation can be described by a Zener-Hollomon parameter with an Arrhenius item, and the constitutive equation of the stress–strain rate can be expressed as follows:

$$\dot{\varepsilon} = 1.987\times10^{12}[\sinh(0.015\,9\sigma)]^{5.821}\exp(\frac{-173\,957.6}{RT}) \quad (8)$$

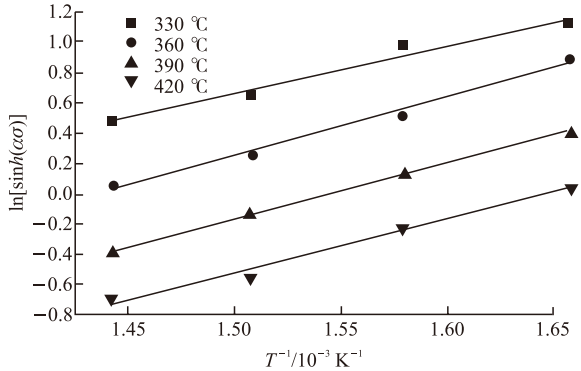

Fig.4 Variation of $\ln[\sinh(\alpha\sigma)]$-$1/T$ at different strain rates, evaluating the averaged apparent activation energy Q

3.3 Microstructural analysis

The optical microstructure of the AZ40 magnesium alloy deformed to a strain level of 0.6 at different deforming temperatures and strain rates is shown in Fig.5. As apparent from Fig.5(a), which was conducted at T = 330 ℃ and = 0.2 s^{-1}, a large number of new fine grains formed around the initial grain boundaries and the second-phase particles because of DRX. High-density dislocations were preferentially formed at the interface between the matrix and the second phases; the nucleation site of DRX was at the grain boundaries and the second-phase boundary. Notably, the deformation twins appeared in the initial coarse grains because of the high strain rate at low deformation temperatures and the limited number of available slip systems, which were the main reasons for the deformation cracks[14]. The as-cast grains were divided by the thin deformation twins and the DRX grains formed inside most of the twins with an average size of approximately 4.6 μm. The post-deformation microstructure has similarities with the AZ serial magnesium alloys reported by Slooff *et al*[15-17].

Fig.5(b) illustrates the microstructure of the specimen deformed at T = 330 ℃ and $\dot{\varepsilon}$= 0.02 s^{-1}, wherein the deformation twins disappeared; the DRX grain sizes increased to approximately 5.8 μm, and no cracks were observed. With increasing deformation temperature, the atomic thermal vibration and the diffusion rate increased; dislocation slipping, climbing, and cross-slipping occurred more easily, and dislocation nodes slipped more easily than at low temperatures. Meanwhile, the nucleation rate of DRX and the ability for grain boundary migration increased with the disappearance of the twins and the grain growth.

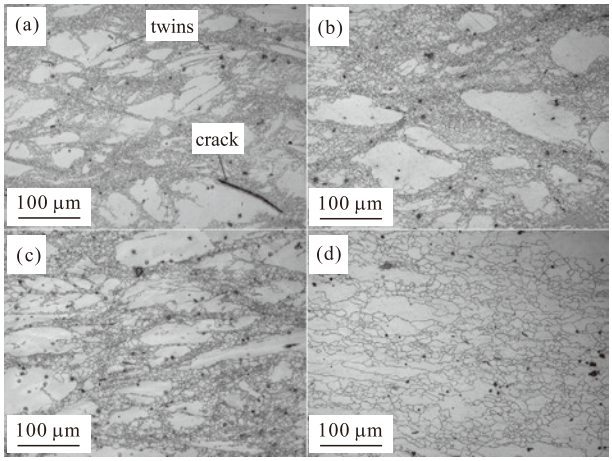

Fig.5 Optical microstructure of the studied alloy deformed to a strain of 0.6 at different deforming conditions: (a) T=330 ℃, $\dot{\varepsilon}$=0.2 s^{-1}; (b) T=330 ℃, $\dot{\varepsilon}$=0.02 s^{-1}; (c) T=390 ℃, $\dot{\varepsilon}$ =0.02 s^{-1}; (d) T=420 ℃, $\dot{\varepsilon}$=0.002 s^{-1}

Fig.5(c) displays the post-deformation microstructure at T = 360 ℃ and $\dot{\varepsilon}$= 0.02 s^{-1}. With increasing temperature, the immigration rate of the recrystallization grain boundaries increases. The DRX grains coarsen to a size of 8.5 μm. The recrystallization zone extends along the direction perpendicular to the compressing direction, which is mainly attributed to the intrinsic anisotropic plasticity of magnesium alloys. With decreasing strain rate, the process of dislocation pile-up slows down; thus, enough time is available for the dislocation recovery, and the stress concentration is eased. As a result, the twins and cracks caused by stress concentration disappear.

Fig.5(d) shows the microstructure of the specimen deformed at T = 420 ℃ and $\dot{\varepsilon}$= 0.002 s^{-1}. Under this deforming condition, the sizes of grains are inclined to be uniform and DRX proceeds completely. According to Galiyev[18], the driving force for grain boundary migration increases with rising temperature; thus, the grain boundary migration rate at 420 ℃ is higher than that at other deforming temperatures, and the average grain size reaches a maximum value of 13.7 μm.

3.4 Processing maps

The processing-map technique has been previously used to study the hot deformation mechanisms in metal materials[19]. The technique of processing maps is based on the dynamic materials

model. The efficiency of power dissipation that occurs through the microstructural changes during deformation is defined as follows:

$$\eta = \frac{2m}{m+1} \tag{9}$$

where, m is the strain rate sensitivity defined by $(\partial \ln\sigma)/(\partial \ln\dot{\varepsilon})$.

As Prasad *et al*[20] mentioned, the extremum principles of irreversible thermodynamics as applied to the continuum mechanics of large plastic flow are explored; these principles define the criteria for the onset of flow instability given by Eq.(10) as follows:

$$\zeta(\dot{\varepsilon}) = \frac{\partial \ln[m(m+1)]}{\partial \ln\dot{\varepsilon}} + m \leqslant 0 \tag{10}$$

the relationship between log (strain rate) and log (stress) can be expressed by function fitting of cubic spline interpolation. Fig.6 shows the flow stress versus the strain rates curves. The material strain rate sensitivity (m) can be determined with Fig.6 and the value of power dissipation efficiency (η) can be calculated with Eq. (9).

The processing maps with different strains (ε=0.3, 0.5, 0.7, and 0.916) are shown in Fig.(7). In the processing maps, the shadow domains stand for the instability regions. Beyond the instability region, the greater the value of η is, the better is the performance of the material processing.

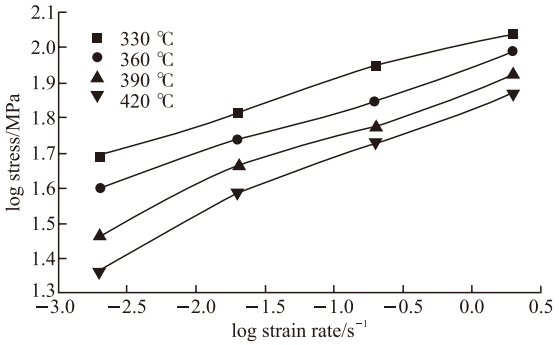

Fig.6 Flow stress *vs*. strain rate data and interpolating curves

No special significant differences were identified between these processing maps. For example, in the processing map with a strain of 0.916, the map exhibits five domains in the temperature and strain rate ranges: (I) T = 330 ℃-350 ℃ and $\dot{\varepsilon}$=1.0-2.0 s^{-1} with a minimum power dissipation efficiency of 12%; (II) T = 330 ℃ and $\dot{\varepsilon}$=0.03 s^{-1} with a peak

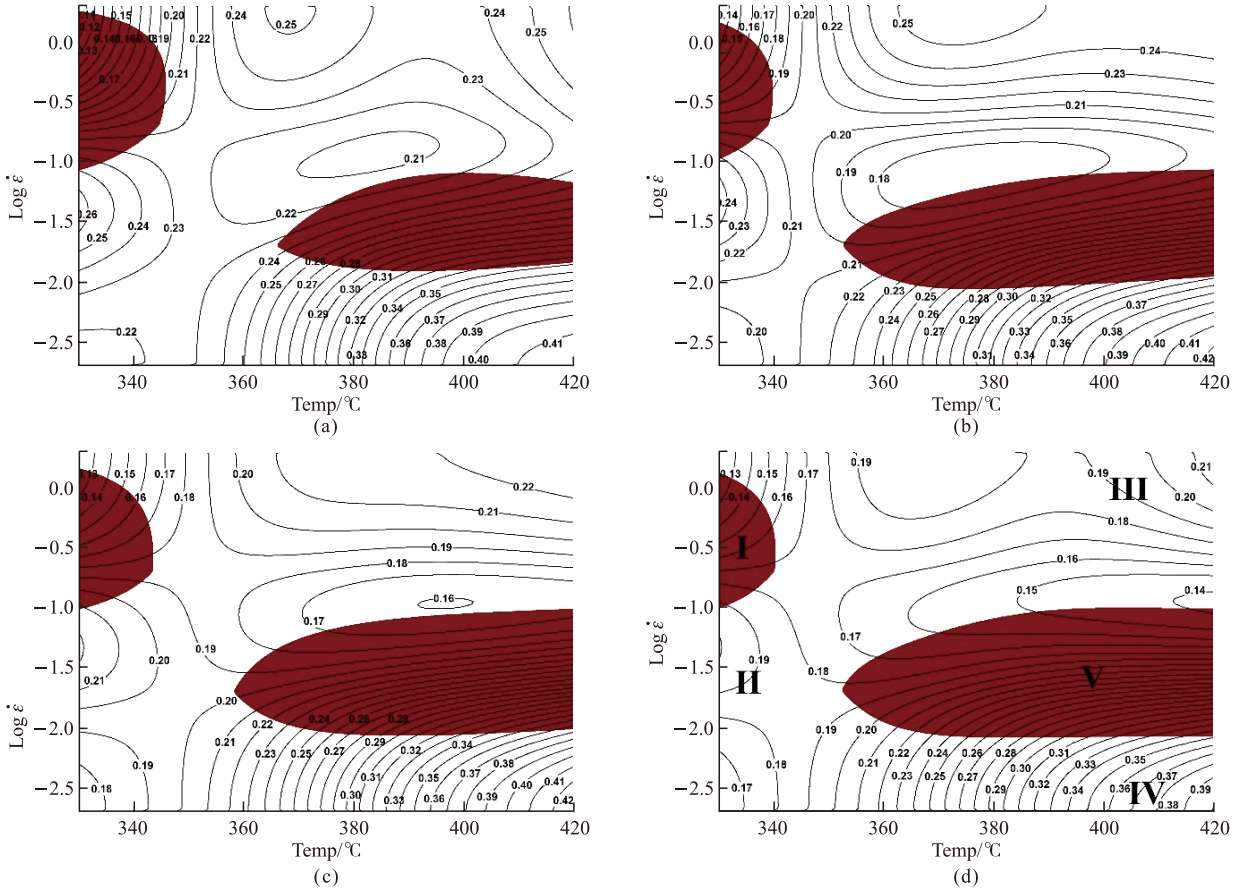

Fig.7 Processing maps at the strain level of (a) 0.3, (b) 0.5, (c) 0.7 and (d) 0.916

efficiency of 20%; (III) T = 360 ℃-420 ℃ and $\dot{\varepsilon}$ =2 s^{-1} with a peak efficiency of 21%; (IV) T = 360 ℃-420 ℃ and $\dot{\varepsilon}$=0.002 s^{-1} with a peak efficiency of 42%; and (V) T = 350 ℃-420 ℃, 0.01-0.1 s^{-1}. The inspection of the microstructure in Fig.5 shows that domain I corresponds to the deformation twins and cracks in Fig.5(a), whereas domains II, III, and IV correspond to a, b, and c, respectively. In domains II and III, the deformation structure presents incomplete recrystallization with negligible DRX grain growth. With the significantly mixed grain structure and the relatively low power dissipation efficiency, the hot deformation performed in domains II or III was not a good choice. In domain IV, the main reason for the high efficiency of power dissipation is the complete DRX and the DRX grain growth. Domain V is a long and narrow area of instability, where the strain rate changes minimally whereas the temperature varies significantly. Results strongly suggest that the AZ40 magnesium alloy deformed in the temperature range of 350 ℃-420 ℃ is highly sensitive to the change of the strain rate. A possible reason may be the change in the proportion of the slip system and DRX during the deformation. A pre-deformation step is advantageous to make recrystallization partially occur before processing. Therefore, a practical process window inferred from Fig. 7 is 360 ℃-420 ℃ and $\dot{\varepsilon}$=0.002 s^{-1}.

4 Conclusions

The hot deformation behavior and microstructural characteristics of the as-cast AZ40 alloy were explored at 330 ℃-420 ℃ and 0.002-2 s^{-1} by hot compression deformation. The following conclusions can be drawn:

a)The flow stress constitutive equation of AZ40 magnesium alloy can be expressed as:

$$\dot{\varepsilon} = 1.987 \times 10^{12}[\sinh(0.015\,9\sigma)]^{5.821}\exp\left(\frac{-173\,957.6}{RT}\right)$$

b) The microstructure of the AZ40 magnesium alloy is highly sensitive to the deformation conditions. At low temperatures with a high strain rate, a large number of twins appeared inside the initial coarse grains, which are the main reason for the mechanical fracture. However, the twins and cracks disappeared after the deformation temperature was increased or the strain rate was decreased.

c)The processing map of the AZ40 alloy at the strain of 0.6 shows three processing domains for hot working: domain II (T = 330 ℃, $\dot{\varepsilon}$= 0.03 s^{-1}), domain III (T = 330-420 ℃, $\dot{\varepsilon}$= 2 s^{-1}), and domain IV (T = 420 ℃, $\dot{\varepsilon}$= 0.002 s^{-1}). In domain IV, the grain sizes tend to be uniform and DRX proceed completely. The results indicate that the optimum hot working condition for the AZ40 magnesium alloy is 420 ℃ and 0.002 s^{-1}.

References

[1] Suresh K, Rao KP, Prasad Y, *et al*. Study of Hot Forging Behavior of As-cast Mg-3Al-1Zn-2Ca Alloy towards Optimization of Its Hot Workability[J]. *Materials & Design*, 2014, 57: 697-704

[2] Agnew SR, Duygulu Ö. Plastic Anisotropy and the Role of Non-basal Slip in Magnesium Alloy AZ31B[J]. *International Journal of plasticity*, 2005, 21(6): 1 161-1 193

[3] Mukai T, Yamanoi M, Watanabe H, *et al*. Ductility Enhancement in AZ31 Magnesium Alloy by Controlling Its Grain Structure[J]. *Scripta Materialia*, 2001, 45(1): 89-94

[4] Yamashita A, Horita Z, Langdon TG. Improving the Mechanical Properties of Magnesium and a Magnesium Alloy through Severe Plastic Deformation[J]. *Materials Science and Engineering: A*, 2001, 300(1): 142-147

[5] Barnett MR. Twinning and the Ductility of Magnesium Alloys: Part I: "Tension" Twins[J]. *Materials Science and Engineering: A*, 2007, 464(1): 1-7

[6] Deng J, Lin YC, Li SS, *et al*. Hot Tensile Deformation and Fracture Behaviors of AZ31 Magnesium Alloy[J]. *Materials & Design*, 2013, 49: 209-219

[7] Fatemi-Varzaneh SM, Zarei-Hanzaki A, Beladi H. Dynamic Recrystallization in AZ31 Magnesium Alloy[J]. *Materials Science and Engineering: A*, 2007, 456(1): 52-57

[8] Fu XS, Chen GQ, Wang ZQ, *et al*. DRX Mechanism of AZ31 Magnesium Alloy during Hot Rolling[J]. *Rare Metal Materials and Engineering*, 2011, 40(8): 1 473-1 477

[9] Srinivasan N, Prasad Y, Rao PR. Hot Deformation Behaviour of Mg-3Al Alloy—A Study Using Processing Map[J]. *Materials Science and Engineering: A*, 2008, 476(1): 146-156

[10] Xu SW, Kamado S, Matsumoto N, *et al*. Recrystallization Mechanism of As-cast AZ91 Magnesium Alloy during Hot Compressive Deformation[J]. *Materials Science and Engineering: A*, 2009, 527(1): 52-60

[11] Wang H, Wang G, Hu L, *et al*. Effect of Hot Rolling on Grain Refining and Mechanical Properties of AZ40 Magnesium alloy[J]. *Transactions of Nonferrous Metals Society of China*, 2011, 21: s229-s234

[12] Lv BJ, Peng J, Wang YJ, *et al*. Dynamic Recrystallization Behavior and Hot Workability of Mg-2.0Zn-0.3Zr-0.9Y Alloy by Using Hot Compression Test[J]. *Materials & Design*, 2014, 53: 357-365

[13] Xia XS, Chen Q, Li JP, *et al*. Characterization of Hot Deformation Behavior of As-extruded Mg-Gd-Y-Zn-Zr alloy[J]. *Journal of Alloys and Compounds*, 2014, 610: 203-211

[14] Li L, Zhang X. Hot Compression Deformation Behavior and Processing Parameters of A Cast Mg-Gd-Y-Zr Alloy[J]. *Materials Science and Engineering: A*, 2011, 528(3): 1 396-1 401

[15] Slooff FA, Dzwonczyk JS, Zhou J, *et al*. Hot Workability Analysis of Extruded AZ Magnesium Alloys with Processing Maps[J]. *Materials Science and Engineering: A*, 2010, 527(3): 735-744

[16] Iwanaga K, Tashiro H, Okamoto H, Shimizu K. Improvement of Formability from Room Temperature to Warm Temperature in AZ-31 Magnesium Alloy[J]. *Journal of Materials Processing Technology*, 2004, 155: 1 313-1 316

[17] Zarandi F, Seale G, Verma R, *et al*. Effect of Al and Mn Additions on Rolling and Deformation Behavior of AZ Series Magnesium Alloys[J]. *Materials Science and Engineering: A*, 2008, 496(1): 159-168

[18] Galiyev A, Kaibyshev R, Gottstein G. Correlation of Plastic Deformation and Dynamic Recrystallization in Magnesium Alloy ZK60[J]. *Acta Materialia*, 2001, 49(7): 1 199-1 207

[19] Prasad V, Sasidhara S. *Hot Working Guide: A Compendium of Processing Maps*[M]. ASM international, 1997: 157-182

[20] Prasad Y, Rao KP. Effect of Homogenization on the Hot Deformation Behavior of Cast AZ31 Magnesium Alloy[J]. *Materials & Design*, 2009, 30(9): 3 723-3 730